

Research Journal of Pharmaceutical, Biological and Chemical Sciences

Spectroscopic And Thermal Investigations Of Olanzapine Drug Charge-Transfer Complexes With Various Acceptors.

Akmal S. Gaballa^{a*}, Sabry A. El-korashy^b, Mahmoud M. Ali^b and Said M. Teleb^c.

^aFaculty of Specific Education, Zagazig University, Zagazig, Egypt

^bChemistry Department, Faculty of Science, Suez Canal University, Ismailia, Egypt

^cChemistry Department, Faculty of Science, Zagazig University, Zagazig, Egypt

ABSTRACT

Interactions of Olanzapine drug (OLP) as electron donor with various electron acceptors as iodine (I₂), picric acid (HPA), chloranilic acid (H₂CA), 2,3-dinitrosalicylic acid (HDNS) and 7,7',8,8' Tetracyanoquinodimethane (TCNQ) were studied in the liquid and solid states. The stoichiometries of all complexes were found to be 1:1 molar ratio between olanzapine and acceptors (I₂, HPA, H₂CA, HDNS and TCNQ). The formed CT-complexes were characterized using UV-Visible spectra, photometric titration measurements, IR and ¹H NMR Spectroscopies as well as Thermal analyses. The characteristic physical constants (*I_D*), (*f*), (*K_{CT}*), (*μ*), (*ΔG*), (*E_{CT}*) of the formed CT-complexes are found to be strongly depend on the kind and structure of the electron acceptors.

Keywords: Charge transfer, Olanzapine, I₂, HPA, H₂CA, HDNS, TCNQ, UV-visible, IR, ¹H NMR, TGA, DTG Spectrometry

<https://doi.org/10.33887/rjpbcs/2019.10.5.14>

**Corresponding author*

INTRODUCTION

Many charge-transfer complexes were formed between electron donor and different type of electron acceptors [1-8]. Charge-transfer complexation has a great worth in bioelectrochemical and biochemical energy-transfer processes [9], systems of biology [10], and drug-receptor binding mechanisms [11]. Studying of drugs CT complexes should be helpful in knowing the mechanisms of action of the drugs [12]. Formation of Charge-transfer complex is also useful in many applications and uses of conductive materials such as in non-linear optical materials [13-16].

2-Methyl-4-(4-methyl-1-piperazinyl)-10H-thieno[2,3-b][1,5]benzodiazepine is the IUPAC name of olanzapine (OLP). Olanzapine drug was approved in 1996 and used in cure of mental illness of teenagers older 13 years of age and adults. The main purposes are to treat schizophrenia, unusual thinking that made by a mental, strong emotional changes and loss of quality of life [17]. Olanzapine has the ability to work as atypical antipsychotic because it makes change in the activity in certain natural substances at the brain. There are two receptor called 5H₂ serotonin receptor and D₂ dopamine receptors where the olanzapine molecule has a high ability to bind for maintaining chemical balance within the brain [18]. Studying the synthesis and spectroscopic characterization of a variety of donor-acceptor complexes is useful to understand the nature of their CT-interaction and its applications [19].

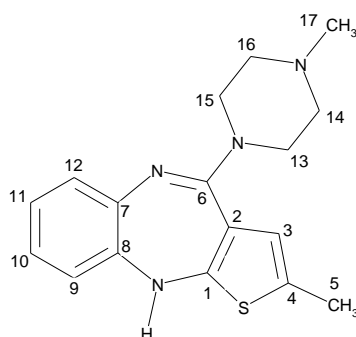
In our work, we report the formation and study of new CT complexes obtained from the reaction of OLP with different electron acceptors, as Iodine, picric acid (HPA), chloranilic acid (H₂CA), 2,3-dinitrosalicylic acid (HDNS) and 7,7',8,8'-tetracyanoquinodimethane (TCNQ) using methanol as a solvent. We used various spectroscopic methods as electronic absorption spectroscopy, infrared (IR), ¹H NMR also elemental analyses and thermal analyses. Finally, we tested the prepared CT complexes against various bacterial as antimicrobial activities.

EXPERIMENTAL

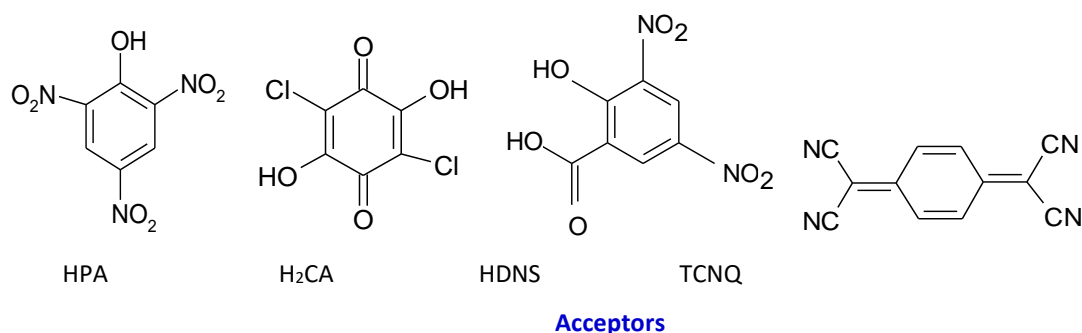
Chemicals

All chemicals we used have high grade (Scheme 1). Olanzapine (OLP) was obtained from Sigma-Aldrich Chemical Co., USA with purity of >98.0%. Iodine (I₂), picric acid (HPA) chloranilic acid (H₂CA) and 2,3-dinitrosalicylic acid (HDNS) and 7,7,8,8-Tetracyanoquinodimethane (TCNQ) were purchased from Merck Chemical Company and used as received.

The electronic absorption spectroscopy was recorded in region of 200-900 nm using UV-Vis. Spectrophotometer model THERMO V-530 with quartz cell of 1.0 cm path length. The infrared spectra of the reactants and the obtained complexes were recorded using KBr discs on TermoFisher Nicolette IS10 Infrared spectrometer. ¹H NMR spectra were recorded using Varian spectrophotometer JEOL ECA-500 II operating at 500 MHz using dimethylsulphoxide-*d*₆ as a solvent and TMS as internal reference.



Donor (OLP)



Scheme 1. Structure of the donor and acceptors

Identification techniques

The microanalyses were carried out at Cairo University using a Perkin-Elmer CHN 2400 (USA). The electronic absorption spectra were carried out in Zagazig University in region range of 200–1000 nm using UV-Vis. Spectrophotometer model THERMO V-530 with quartz cell of 1.0 cm path length. The infrared spectra of the reactants and complexes were carried out at Mansoura University using KBr discs on TermoFisher Nicolette IS10 Infrared spectrometer. ¹H NMR spectra carried out at Mansoura University using a Varian spectrophotometer JEOL ECA-500 II operating at 500 MHz using dimethylsulphoxide-d₆ as a solvent and TMS as internal reference. Thermal analyses were carried out in the STCE Center of the Egyptian Ministry of Military Production. Finally, biological activities were carried out at the micro lab of Cairo University.

Spectrophotometric titration measurements

Photometric titrations measurements for the reactions between OLP and the defined acceptors were done at the CT absorption bands (360), (354), (305), (310) and (350, 810 nm) for complexes **1**, **2**, **3**, **4**, and **5**, respectively. A 0.25, 0.50, 0.75, 1.00, 1.25, 1.5, 2.00, 2.50, 3.00 or 3.50 mL aliquot of a standard solution (1.0×10^{-4} M) of the appropriate acceptor in MeOH was added to 1.00 mL of 1.0×10^{-4} M OLP, which was also dissolved in MeOH. The total volume of the mixture was 5 mL. the concentration of the acceptors (C_a) ranged with concentrations (0.25×10^{-4} M to 3.5×10^{-4} M), where concentration of OLP (C_d) in the reaction mixture was maintained at 1.00×10^{-4} M to produce solutions with an acceptor molar ratio that varied from 0.25:1.00 to 1.00:3.5. The stoichiometries of the molecular CT complexes were then obtained using the known method [20].

Syntheses of the solid complexes

The solid $[(\text{OLP})_2]^{+} \cdot \text{I}_3^{-}$ (**1**), $[(\text{HOLP})(\text{PA})]$ (**2**), $[(\text{HOLP})(\text{HCA})]$ (**3**), $[(\text{HOLP})(\text{DNS})]$ (**4**) and $[(\text{OLP})(\text{TCNQ})]$ (**5**) complexes were prepared by adding a saturated (30 mL) of Methanol solution of (1.00 mmol) the acceptors to (10 mL) of methanolic solution of the donor OLP (1.00 mmol). The resultant dark brown, scarlet-yellow, dark violet, dark yellow and dark green solutions of complexes **1– 5**, separately were stirred for 2h at room temperature then left overnight to separate the solid complexes. The precipitate of complexes were filtrated off, washed three times with MeOH and then dried in vacuole overnight over CaCl₂.

$[(\text{OLP})_2]^{+} \cdot \text{I}_3^{-}$ (**1**): Anal. found (Calcd. for $\text{C}_{17}\text{H}_{20}\text{I}_4\text{N}_4\text{S}$, 820.05): C, 24.43 (24.90); H, 2.48 (2.46); N, 6.88 (6.83); S, 3.90 (3.91).

$\delta = 2.31$ [s, 3H, (CH₃)], 2.49 [s, 3H, (CH₃)], 2.89 [m, 4H, (CH₂)], 3.37 [m, 4H, (CH₂)], 6.68 [s, 1H, (CH)] 6.90-7.20 [m, 4H (CH)], 9.8 [s, 1H, (NH)].

$[(\text{HOLP})(\text{PA})]$ (**2**): Anal. found (Calcd. for $\text{C}_{23}\text{H}_{23}\text{N}_7\text{O}_7\text{S}$, 541.54): C, 50.06 (51.01); H, 4.31 (4.28); N, 19.12 (18.11); S, 5.95 (5.92).

$\delta = 2.26$ [s, 3H, (CH₃)], 2.49 [s, 3H, (CH₃)], 2.79 [m, 4H, (CH₂)], 3.20 [m, 4H, (CH₂)], 6.41 [s, 1H, (CH)] 6.71-6.88 [m, 4H, (CH)], 7.89 [br, 1H, (NH⁺)], 8.58 [(s, 2H, (H₃/H₅, PA)].

[(HOLP)(HCA)] (3): Anal. found (Calcd. for $C_{23}H_{22}N_4Cl_2O_4S$, 521.43): C, 52.12 (52.97); H, 34.29 (4.25); N, 10.52 (10.74); S, 6.32 (6.14).

δ = 2.26 [s, 3H, (CH₃)], 2.49 [s, 3H, (CH₃)], 2.80 [m, 4H, (CH₂)], 3.20 [m, 4H, (CH₂)], 3.60 [br, 1H, (NH⁺)], 6.41 [s, 1H, (CH)] 6.72-6.92 [m, 4H (CH)], 7.96 [(br, 1H, (OH, HCA))].

[(HOLP)(DNS)] (4): Anal. found (Calcd. for $C_{24}H_{24}N_6O_7S$, 540.55): C, 53.62 (53.32); H, 4.51 (4.47); N, 15.31 (15.54); S, 5.82 (5.93).

δ = 2.26 [s, 3H, (CH₃)], 2.49 [s, 3H, (CH₃)], 2.69 [m, 4H, (CH₂)], 3.05 [m, 4H, (CH₂)], 3.50 [br, 1H, (NH⁺)], 6.32 [s, 1H, (CH)] 6.68-6.87 [m, 4H (CH)], 7.78 [(br, 1H, (OH, DNS))], 8.30 [(s, 1H, (2CH, DNS))]

[(OLP)(TCNQ)] (5) Anal. found (Calcd. for $C_{29}H_{24}N_8S$, 516.62): C, 66.13 (67.42); H, 4.66 (4.68); N, 21.81 (21.68); S, 6.23 (6.20).

δ = 2.26 [s, 3H, (CH₃)], 2.49 [s, 3H, (CH₃)], 2.82 [m, 4H, (CH₂)], 3.36 [m, 4H, (CH₂)], 6.36 [s, 1H, (CH)] 6.60-6.90 [m, 4H (CH)], 7.74-7.92 [(d, 4H, (4CH, TCNQ))], 8.3 [s, 1H, (NH⁺)].

Biological assessment

In vitro against bacterial strains (*Pseudomonas aeruginosa*, *Staphylococcus aureus*, *Bacillus subtilis*, and *Escherichia coli*), newly synthesized CT complexes and the pure solvent were tested using the agar well diffusion method. The CT-complex samples and standards were dissolved in DMSO to make concentrations of 100 μ g/mL. The inoculum (1×10^8 CfU/mL) was added to molten agar and the media were shaken to disperse the microorganisms. In the agar with a sterile cork borer, four millimeters diameter wells were punched. A 10 μ L of the CT-Complexes were introduced in the well. The diameters of inhibition zone were measured in mm to determine the antimicrobial activity [21, 22].

RESULT AND DISCUSSION

Electronic spectra

Electronic absorption spectra of the donor OLP and of the formed CT-complexes are shown in Fig. 1. These detected new strong absorption bands refer to the CT-interactions. These bands are not present in the spectra of the free reactants and are observed at (360), (354), (305), (310), (350, 810 nm) for the complexes, [(OLP)₂I₃]⁺ and [(HOLP)(PA)], [(HOLP)(HCA)], [(HOLP)(DNS)] and [(OLP)(TCNQ)], respectively.

Photometric titration measurements based on these characteristic CT-absorption bands of the CT-complexes, Fig. 2, confirmed the complex formation in a ratio, OLP: acceptor of 1:1 in all cases. Here, we indicate that the observed relative OLP-acceptor molar ratios compared with those known for other related donor-acceptor systems could be refer to the relatively high steric effects of the systems under investigations [23]. The obtained spectrophotometric data, Tables 1 and 2 were used to calculate the values of both equilibrium constants, K_{CT} , and extinction coefficient, ϵ of the formed CT-complexes in MeOH based on the known equation (1) for the 1:1 stoichiometry [24].

$$\frac{C_d^{\circ} \cdot C_a^{\circ}}{A} = \frac{1}{\epsilon K_c} + \frac{C_d^{\circ} + C_a^{\circ}}{\epsilon} \quad (1)$$

where C_d° and C_a° are the initial concentration of the acceptors (I₂, HPA, H₂CA, DNS, TCNQ) and the OLP donor and A is the absorbance of the strong CT band at 360, 305, 310 and (350, 810 nm) for the complexes 1–5, respectively. When $C_d^{\circ} \cdot C_a^{\circ}/A$ are plotted against $(C_d^{\circ} + C_a^{\circ})$, straight lines are obtained with a slope of $1/\epsilon$ and intercept of $1/\epsilon K_c$, Fig. 3.

The spectroscopic and physical data are summarized in Table 3 such as the ionization potential (I_D) oscillator strength (f), standard free energy (ΔG°), were estimated for complexes dissolved in methanol at room temperature. The oscillator strength (f) can be calculated by equation 2 [25].

$$f = 4.319 \times 10^{-9} (\epsilon_{\max} \cdot \Delta\nu_{1/2}) \quad (2)$$

The transition dipole moments (μ) of the OLP CT- complexes have been calculated according to equation 3 [26].

$$\mu_{(Debye)} = 0.958 \left(\frac{\epsilon_{\max} \cdot \Delta\nu_{1/2}}{\nu_{\max}} \right)^{1/2} \quad (3)$$

Aloisi and Pignataro equation (4) is used to calculate the ionization potentials (I_D) of the OLP donor in the CT complexes [27].

$$I_{D(eV)} = 5.76 + 1.53 \times 10^{-4} \cdot \nu_{CT} \quad (4)$$

Briegleb equation (5) is used to calculate the energy values (E_{CT}) of the n to π^* and π - π^* interactions between the donor (OLP) and the acceptors [28].

$$E_{CT} = (h\nu_{CT}) = 1243.667 / \lambda_{CT(nm)} \quad (5)$$

The standard free energy of CT-complexation (ΔG° , kJmol^{-1}) for each complex was calculated using equation 6 [29].

$$\Delta G^\circ = -2.303 RT \log K_{CT} \quad (6)$$

where R is the gas constant ($8.314 \text{ J mol}^{-1} \text{ K}$), T is the temperature in Kelvin degrees ($273 + ^\circ\text{C}$) and K_{CT} is the formation constant of the complexes (l mol^{-1}) at room temperature.

The calculated spectroscopic and physical values (f , μ , I_D , and ΔG°) for the obtained CT complexes using these equations are presented in Table 3. [(HOLP)(HCA)] and [(OLP)(TCNQ)] complexes exhibit considerably higher values of both the oscillator strength (f) and the transition dipole moment (μ). The observed high values of f refer to a strong interaction between the donor-acceptor pairs with relatively high probabilities of CT-transitions [30]. The obtained values of ΔG° for the [(OLP) $_2$ l] $^{+} \cdot \text{l}_3$, [(HOLP)(PA)], [(HOLP)(HCA)], [(HOLP)(DNS)] and [(OLP)(TCNQ)] complexes are (-2.14), (-2.42), (-2.39), (-2.31) and (-2.33, -2.72). kJmol^{-1} , respectively. These negative values indicate that the interaction between the drug and acceptors is exothermic and spontaneous [31, 32].

IR Spectra

The vibrational spectral free donor, olanzapine drug and synthesized complexes are represented in Fig 4 and the characteristic of these assignments are given in Table 4. The formation of CT- complexes during the reaction of OLP with l_2 , HPA, H_2CA HDNS and TCNQ is supported by observing of main infrared bands of free donor (OLP) and acceptors (l_2 , HPA, H_2CA , HDNS, TCNQ) in the product spectra. It is worth mentioning that these bands are changed both in intensity and frequency values as a result of expected change in electronic structure upon complexation.

In case of [(OLP) $_2$ l] $^{+} \cdot \text{l}_3$, small shifts occurred to N-H from 3221 cm^{-1} to 3432 cm^{-1} , C-O from 1178 cm^{-1} to 1231 cm^{-1} and C-N from 1222 cm^{-1} to 1238 cm^{-1} . In the state of interaction between acid and base, a transfer of proton from the acceptor (acid) to the donor (base) is expected to occur. This seems to be occurring in the case of OLP interaction with 2,3-dinitrosalicylic, chloranilic and picric acids. That is strongly upholder by the appearance of a new band of medium intensity in the complex spectra. This band is observed at 3323 cm^{-1} for OLP-HDNS, 3425 cm^{-1} for OLP- H_2CA CT-complex and at 3533 cm^{-1} for OLP-HPA CT-complexes which might

be due to the stretching vibration of hydrogen from (N–H) group against positively charged nitrogen. We may suggest that, the acid–base interaction is followed with a proton migration with hydrogen bond formation. The OLP–HDNS, OLP–H₂CA and OLP–HPA interaction involves a protonation for the lowest basic nitrogen of the OLP nitrogens, Accordingly, we may formulate the complexes as [(HOLP)(DNS)], [(HOLP)(HCA)], [(HOLP)(HPA)] [33]. The IR spectrum of TCNQ shows CN stretching frequency at 2222 cm⁻¹. The significant shift of this vibration towards lower frequency to 2181 cm⁻¹ in the complex spectrum, [(OLP)(TCNQ)], indicates that charge transfer take place from π (OLP) \rightarrow π^* (TCNQ) of a CN group, leads to increasing the anti-bonding electrons of the CN group, weakens the C–N bond and hence the observed shift to lower frequency [34].

¹H NMR spectra

The nuclear magnetic resonance spectra, Fig 5 present the persuasive confirmation of the complexation pathway. Thus, the 500 MHz ¹H NMR spectra of the OLP CT-complexes were measured in dmsod₆ at room temperature. The chemical shifts (δ) of the different types of protons of the CT complexes are summarized in Table 5.

For complex 1 [(OLP)₂]⁺·I₃⁻, the NH signals are shifted to 9.80 and all of the other peaks are located in the same region as in free OLP and in the iodine complex, except two CH signals [35].

In the ¹H NMR spectrum of complex 2 [(HOLP)(PA)], the new broadened signal was observed at 7.8 ppm which is not detected in the spectrum of the free OLP donor and is attributed to the formation of Hydrogen bond between HPA and OLP. The signal at 11.94 ppm is assigned to the OH proton of free picric acid, was absent in the spectrum of this complex. Together, these data indicated that the amino and phenolic groups are involved in the formation of the CT complex between OLP and HPA [36]. The presence of a signal at 8.58 ppm referred to the two protons of picric acid ring.

For complex 3 [(HOLP)(HCA)], it was observed that a new large broad signal at 3.71 ppm attributing to the protons of NH⁺₂. This situation confirmed the transfer of the phenolic proton of H₂CA to the amino group (-NH) of OLP and presence of new signal at 7.90 ppm that referred to (OH) group of chloranilic acid [37].

For complex 4 [(HOLP)(DNS)], the proton of COOH signal of free acceptor (DNS) disappeared in the spectrum of its CT complex, This means the involvement of COOH group in chelating through the deprotonation from the acceptor to donor. A new large broad signal is observed at 3.50 ppm attributing to two protons of NH⁺₂. This situation confirmed the transfer of the proton carboxyl group of HDNS to the amino group (-NH) of OLP and presence of new signal at 7.78 ppm referred to (OH) group of HDNS [38].

In the ¹H NMR spectrum of complex 5 [(OLP)(TCNQ)] confirmed that the (-NH) and (-C≡N) groups are primarily involved in the formation of the CT complex between OLP and TCNQ. The migration of the H⁺ ion from the NH group in the OLP donor to cyano groups in the TCNQ acceptor resulted in the formation of the positive ion (-C≡N⁺H), which is associated with the anion (O⁻). This result was also confirmed from the disappearance of the (NH) signal in the spectrum of CT complex and a new signal appeared at 8.30 ppm due to the formation of hydrogen bond between OLP and TCNQ [39]. The presence of two new signals between 7.74 and 9.42 ppm are attributed to the four H protons of TCNQ.

Thermal analysis

The proposed structures for the complexes under investigation were confirmed by measuring TGA, and DTG thermograms (Fig 6) under nitrogen flow. The thermal data obtained for complexes 1–5 together with the free donor, OLP are summarized and given in Table 6.

The free OLP decomposes in one stage at 286°C. The total weight loss associated with this step of decomposition is near to the theoretical calculation.

For [(OLP)₂]⁺·I₃⁻ complex, decomposition reactions occur in two stages at 248 and 314 °C with a weight loss of 16.13% and 61.9%, respectively. These values of weight loss may be due to the loss of OLP and iodine moieties in good agreement with the calculated values of 16.06% and 62.21%, respectively. The decomposition of the complex molecule ended with final residual carbon atoms [40].

In case of [(HOLP)(PA)] (**2**), the decomposition reactions occur in one stage at T_{\max} 225 °C with a weight loss of 82.27%. These values of weight loss may be due to the loss of HOLP and PA moieties in good agreement with the calculated values of 82.71%. The decomposition of the picrate complex molecule ended with final residual carbon atoms [41].

For [(HOLP)(HCA)] (**3**), the decomposition reactions occur in two stages at T_{\max} 161 and 248 °C with a weight loss of 10.18% and 61.16%, respectively. These values of weight loss may be due to the loss of HOLP and HCA moieties in good agreement with the calculated values of 10.35% and 60.99%, respectively. The decomposition of the complex molecule ended with final residual carbon atoms [42].

In [(HOLP)(DNS)] (**4**) thermogram, the decomposition reactions occur in two main stages at 83 and 234 °C with a weight loss of 7.03 and 52.95%. These values of weight loss may be due to the loss of OLP and HDNS moieties in good agreement with the calculated values of 7.00 and 52.54%, respectively. The final residue of decomposition steps is carbon atoms [43].

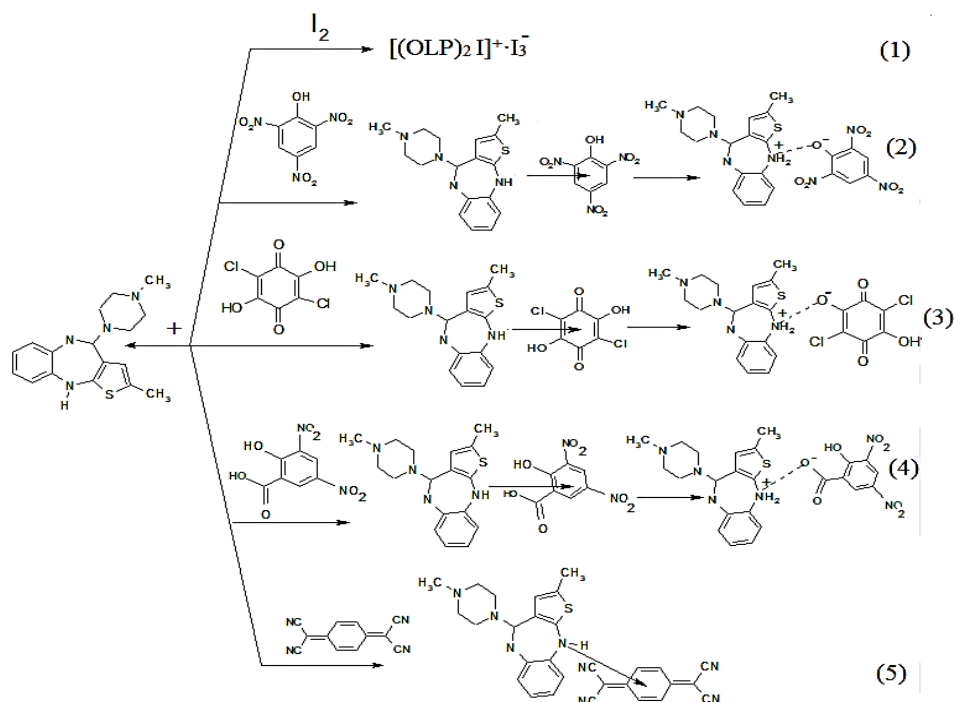
In case of [(OLP)(TCNQ)] (**5**), the decomposition reactions occur in two stages around 137 and 345 °C with a weight loss of 13.95 and 43.41%. These values of weight loss may be due to the loss of OLP and TCNQ moieties in good agreement with the calculated values of 13.90 and 44.00%, respectively. The decomposition of the complex molecule ended with final residual carbon atoms [44].

Antibacterial activities

Two Gram-positive bacterial strains as *Staphylococcus aureus* (*S. aureus*) and *Bacillus subtilis*, and two Gram-negative bacterial strains, *Escherichia coli* (*E. coli*) and *Pseudomonas aeruginosa* (*P. aeruginosa*) are used to test antibacterial activity of the prepared CT complexes. The measuring of inhibition zone diameter values (mm) of the complexes against the microorganisms activity could determine. The positive control was ampicillin. The data are recorded in Table 7. The results indicated that the olanzapine CT-complexes have medium inhibition results against all of the gram-positive and gram-negative bacterial species. The antibacterial activities of standard ampicillin are higher than all the CT-complexes and complex **1** have higher antibacterial activity than other complexes.

CONCLUSION

Charge transfer interactions accrued between the donor (OLP) and σ acceptor like I_2 and π -acceptors as HPA, H_2CA , HDNS and TCNQ were studied in MeOH at 25°C. We were able to show that the synthesized CT complexes were characterized using various spectroscopic techniques including UV-Visible, IR, 1H NMR spectroscopies and thermal analysis. We observed that the reaction stoichiometry is 1:1 for all acceptors I_2 , HPA, H_2CA , HDNS and TCNQ. The resulting CT-complexes were shown to have the formulas: [(OLP) $_2I_2$] (**1**), [(HOLP)(PA)] (**2**), [(HOLP)(HCA)] (**3**), [(HOLP)(DNS)] (**4**) and [(OLP)(TCNQ)] (**5**). The obtained complexes are semi-crystalline material and thermally stable. Physical parameters such as formation constant (K_{CT}), molar extinction coefficient (ϵ_{CT}) and other spectroscopic have been estimated. We concluded that the charge transfer reaction of olanzapine (OLP) as a donor with various acceptors take place in a molar ratio of 1:1 according to Scheme 2 as follows:



Scheme 2. Proposed CT-complexes of olanzapine (OLP) with different electron acceptors

Table 1. The values of $C_d^{\circ}, C_a^{\circ}/A$ and $C_d^{\circ} + C_a^{\circ}$ for complexes 1–3

$C_d^{\circ} \times 10^{-4}$	$C_a^{\circ} \times 10^{-4}$	Ratio (a/d)	$C_d^{\circ} + C_a^{\circ} \times 10^{-4}$	$C_d^{\circ} \cdot C_a^{\circ} \times 10^{-8}$	Complex 1		Complex 2		Complex 3	
					A	$C_d^{\circ} \cdot C_a^{\circ} / A$	A	$C_d^{\circ} \cdot C_a^{\circ} / A$	A	$C_d^{\circ} \cdot C_a^{\circ} / A$
					360	$\times 10^{-8}$	354	$\times 10^{-8}$	305	$\times 10^{-8}$
1	0.25	0.25	1.25	0.25	0.309	0.810	0.482	0.525	0.073	17.36
1	0.50	0.50	1.50	0.50	0.519	0.963	0.803	0.617	0.138	10.86
1	0.75	0.75	1.75	0.75	0.896	0.842	1.013	0.694	0.176	9.946
1	1.00	1.00	2.00	1.00	1.252	0.801	1.572	0.636	0.241	8.294
1	1.25	1.25	2.25	1.25	1.421	0.882	1.831	0.683	0.251	8.965
1	1.50	1.50	2.50	1.50	1.612	0.931	2.371	0.738	0.252	9.924
1	2.00	1.75	3.00	2.00	1.873	1.069	2.202	0.904	0.257	11.67
1	2.50	2.00	3.50	2.50	1.916	1.315	2.611	0.988	0.258	13.56
1	3.00	2.50	4.00	3.00	2.170	1.382	2.860	1.112	0.268	14.92
1	3.50	3.00	4.50	3.50	2.251	1.555	3.232	1.245	0.269	16.72

Table 2. The values of $C_d \cdot C_a / A$ and $C_d + C_a$ for complexes 4 and 5

$C_d \times 10^{-4}$	$C_a \times 10^{-4}$	Ratio (a/d)	$C_d + C_a \times 10^{-4}$	$C_d \cdot C_a \times 10^{-8}$	Complex 5		Complex 5		Complex 4	
					A	$C_d \cdot C_a / A$	A	$C_d \cdot C_a / A$	A	$C_d \cdot C_a / A$
					810	$\times 10^{-8}$	350	$\times 10^{-8}$	310	$\times 10^{-8}$
1	0.25	0.25	1.25	0.25	0.088	2.842	0.35	0.714	0.490	2.551
1	0.50	0.50	1.50	0.50	0.162	3.081	0.7	0.712	1.312	1.145
1	0.75	0.75	1.75	0.75	0.241	3.121	1.29	0.571	1.426	1.230
1	1.00	1.00	2.00	1.00	0.358	2.795	1.6	0.625	2.054	0.975
1	1.25	1.25	2.25	1.25	0.378	3.316	1.7	0.735	2.152	1.046
1	1.50	1.50	2.50	1.50	0.394	3.848	1.83	0.819	2.513	0.996
1	2.00	1.75	3.00	2.00	0.412	4.852	2.1	0.952	2.715	1.107
1	2.50	2.00	3.50	2.50	0.464	5.381	2.23	1.121	2.914	1.206
1	3.00	2.50	4.00	3.00	0.494	6.072	2.65	1.132	3.048	1.315
1	3.50	3.00	4.50	3.50	0.512	6.835	3.06	1.143	3.061	1.470

Table 3. Spectrophotometric results for the prepared CT-complexes in MeOH

Complex	λ_{\max} (nm)	K_c ($l \cdot mol^{-1}$)	ϵ_{\max} ($l \cdot mol^{-1} \cdot cm^{-1}$)	E_{CT} (eV)	F	μ	I_D (ev)	$\Delta G^\circ(25^\circ C)$ ($K \cdot J \cdot mol^{-1}$)
Complex 1	360	1.25×10^4	1.01×10^4	3.454	12.96	31.23	11.02	-2.14×10^4
Complex 2	354	$.77 \times 10^4$	5.20×10^4	3.513	28.07	45.95	10.59	-2.42×10^4
Complex 3	305	$.92 \times 10^4$	0.33×10^4	4.01	52.92	22.375	10.73	-2.39×10^4
Complex 4	310	$.66 \times 10^4$	1.50×10^4	4.07	25.91	50.32	10.02	-2.31×10^4
Complex 5	350	2.8×10^4	1.00×10^4	3.55	58.32	97.06	10.42	-2.23×10^4
	810	1.72×10^4	0.77×10^4	1.483	19.00	58.17	9.58	-2.72×10^4



Table 4. Characteristic infrared frequencies (cm^{-1}) and tentative assignments for OLP and its CT-complexes

OLP	HPA	H ₂ CA	DNS	TCNQ	Complex 1	Complex 2	Complex 3	Complex 4	Complex 5	Assignments
3221br	3416 br	3235w	3572br 3450br		3432br 3215m	3533vs 3347br	3425vbr	3323 vs.br	3445s.br	v(N-H), v (O-H) H bonded
3055			3104 s	3137 ms		3022m	2957mbr	3011 vs	3261 m	v(C-H) Aromatic
2985m 2961m	2980sh 2872w		2854mr	2969 w 2220s	2922w	2861w		2922 m	2933 m 2181s	v _s (C-H) + v _{as} (C-H) v(C≡N),
	1636 vs		1820 s			1561 vs		1708 s		v _{as} (NO ₂)
1557s 1467s	1610 ms	1368vs	1609 s	1404s	1620vs	1623s 1593vs	1630vs	1592m	1595 s	v(C=C) stretch,
1287 m 1357m			1528 s		1423m	1406m 1362s	1594m 1376m	1520 s	1365 s 1345 m	(C-H) Plane bending
1222 s 1178s	1312ms 1150ms	1369m 1290vs	1395w 1341m	1352 ms 1117ms	1238 m 1231m	1275s 1331m	1283 s 1238m	1282 s 1215 m	1283m 1184m	v(C-N) v(C-O)
	1150ms		819 w			1292m				v _s (NO ₂), PA
						1156 s	971s	966 s		(NH ₂ ⁺) Complexes
782s		690m	703s	860s	735vw	985m	836m	933s	825m	CH ₂ Rocking

*: s, strong; w, weak; m, medium; sh, shoulder; v, very; br, broad.

**Table 5.** ^1H NMR δ values (ppm) for OLP and its CT-complexes in $\text{dms}\text{-d}_6$

Compound	C^5H_3 D	C^{17}H_3 D	$\text{C}^{13,16}\text{H}_2$ D	$\text{C}^{14,15}\text{H}_2$ D	C^3H D	$\text{C}^{9,10,11,12}\text{H}$ D	NH D	NH^{2+} D	4CH TCNQ	OH CA	NH^+	H3/H5 PA	H3/H5 DNS	OH DNS
D	2.25	2.34	2.49	3.34	6.63	6.68-6.83	7.59							
1	2.31	2.49	2.89	3.37	6.68	6.90-7.20	9.80							
2	2.26	2.49	2.79	3.20	6.41	6.71-6.88		7.89				8.588		
3	2.26	2.49	2.80	3.24	6.43	6.62-6.92		3.71		7.90				
4	2.26	2.49	2.69	3.05	6.32	6.68-6.89		3.50					8.65 8.67	7.78
5	2.26	2.49	2.82	3.36	6.36	6.68-6.86			7.74 7.94		8.30			

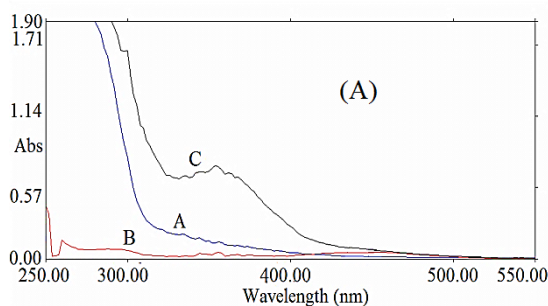
Table 6. The maximum temperature values for the decomposition along with the species lost in each step of the decomposition reaction of the free OLP and its CT-complexes

Complex	Decomposition	$T_{max}/^{\circ}\text{C}$	Lost species	% Weight loss	
				Found	Calc.
OLP	First stage	286	$\text{C}_{17}\text{H}_{20}\text{N}_4\text{S}$	100.00	99.77
	Residue			00.00	00.23
[(OLP) ₂ I] ⁺ ·I ₃ ⁻ (1)	First main stage	248	$\text{C}_2\text{H}_{20}\text{N}_4\text{S}$	16.13	16.06
	Second stage	314	I ₄	61.91	62.21
	Residue	380	Carbon residue	21.96	21.73
[(HOLP)(PA)] (2)	First stage	225	$\text{C}_{15}\text{H}_{23}\text{N}_7\text{O}_7\text{S}$	82.27	82.71
	Residue		Carbon residue	17.73	17.29
[(HOLP)(HCA)] (3)	First step	161	CH_{13}N_2	10.35	10.18
	Second step	248	$\text{C}_5\text{H}_9\text{N}_2\text{Cl}_2\text{O}_4\text{S}$	61.16	60.99
	Residue		Carbon residue	28.49	28.58
[(OLP)(DNS)] (4)	First stage	83	C_2N	7.35	7.00
	Second stage	234	$\text{C}_6\text{H}_{24}\text{N}_5\text{O}_7\text{S}$	52.95	52.54
	Residue		Carbon residue	39.70	40.46
[(OLP)(TCNQ)] (5)	First stage	137	CN_2S	13.95	13.90
	Second stage	345	$\text{C}_{10}\text{H}_{24}\text{N}_6$	43.41	44.00
	Residue		Carbon residue	42.64	43.00

Table 7. Antibacterial activity (inhibition zone diameter in mm) for the CT-complexes of OLP

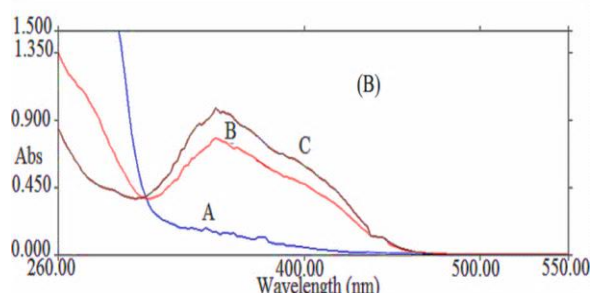
Sample	Bacteria			
	<i>Bacillus subtilis</i> , G ⁺	<i>Staphylococcus aureus</i> , G ⁺	<i>Esherichia coli</i> , G ⁻	<i>Pseudomonas aeruginosa</i> , G ⁻
DMSO	0.0	0.0	0.0	0.0
Ampicilin	18	18	22	17
Complex 1	15	13	14	16
Complex 2	11	11	12	11
Complex 3	0.0	0.0	0.0	0.0
Complex 4	9	16	10	15
Complex 5	0.0	0.0	0.0	0.0

Fig 1. Elecectronic absorption spectra of :



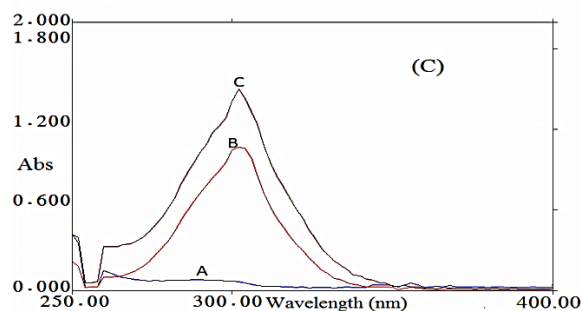
(A) : OLP-I₂ reaction in MeOH

(a) : ([OLP] = 1×10^{-4} M, (b) : [I₂]= 1×10^{-4} M and (c) : [OLP-I₂ product] = 1×10^{-4} M



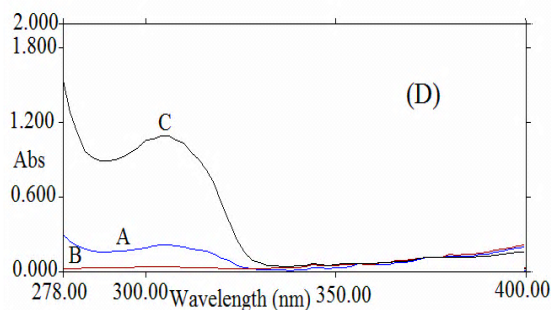
(B) : OLP-HPA reaction in MeOH

(a) : ([OLP] = 1×10^{-4} M, (b) : [HPA]= 1×10^{-4} M and (c) : [OLP-HPA product] = 1×10^{-4} M



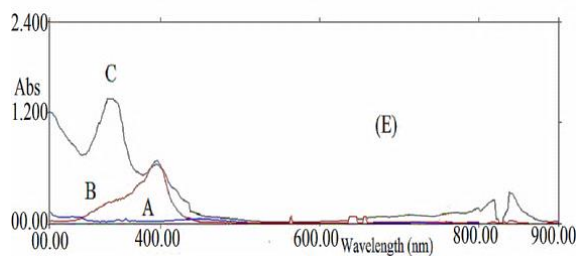
(C) : OLP-H₂CA reaction in MeOH

(a) : [OLP] = 1×10^{-4} M, (b) : [H₂CA]= 1×10^{-4} M and (c) : [OLP-H₂CA product] = 1×10^{-4} M



(D) : OLP-DNS reaction in MeOH

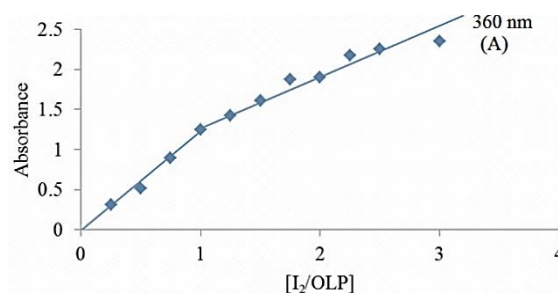
(a) : ([OLP] = 1×10^{-4} M, (b) : [DNS]= 1×10^{-4} M and (c) : [OLP -DNS product] = 1×10^{-4} M



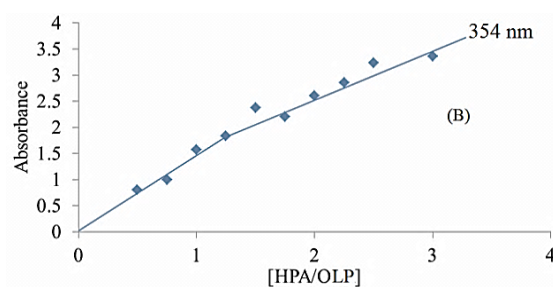
(E) :OLP-TCNQ reaction in MeOH

(a) : ([OLP] = 1×10^{-4} M, (b) : [TCNQ] = 1×10^{-4} M and (c) : [OLP-TCNQ product] = 1×10^{-4} M

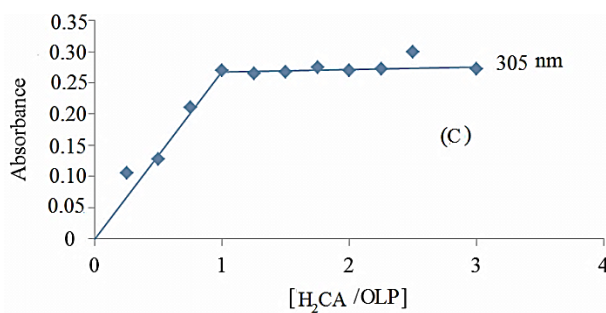
Fig 2. Photometric titration curves of :



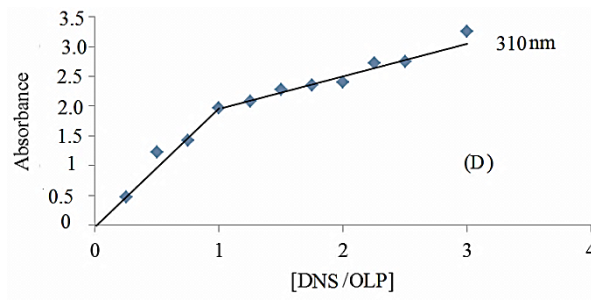
(A): OLP-I₂ reaction in MeOH at 360 nm



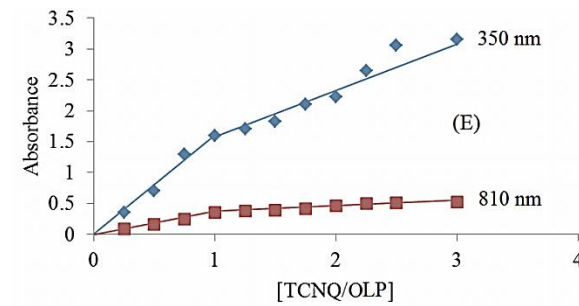
(B): OLP-HPA reaction in MeOH at 354 nm



(C): OLP-H₂CA reaction in MeOH at 305 nm

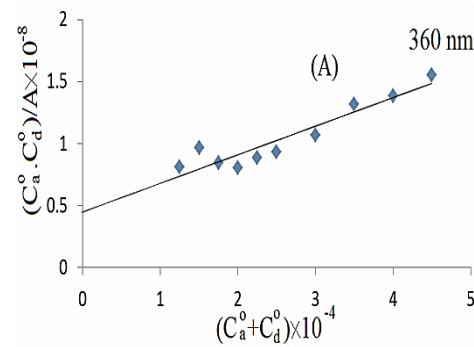


(D): OLP-DNS reaction in MeOH at 460 nm

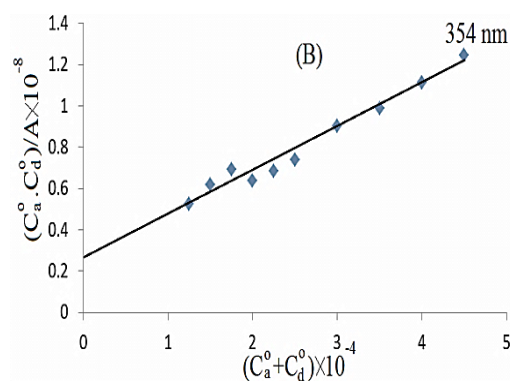


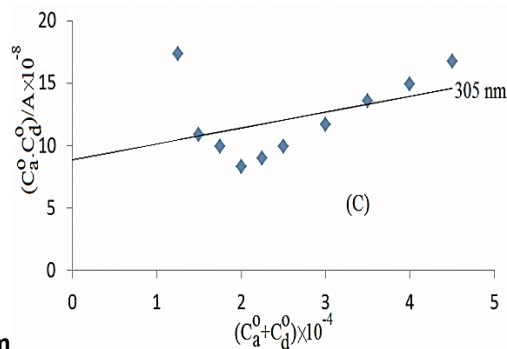
(E): OLP-TCNQ reaction in MeOH at 350 nm and 810 nm

Fig 3. Relation between $C_d^o \cdot C_a^o / A$ and $C_d^o + C_a^o$ for:



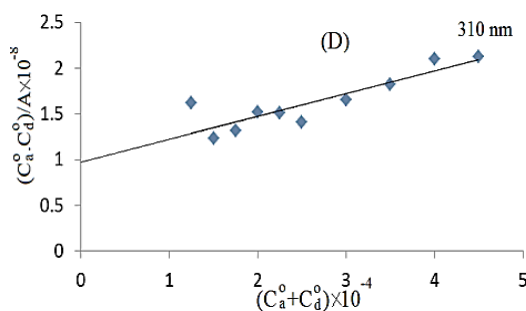
(A): OLP-I₂ reaction in MeOH at 360 nm



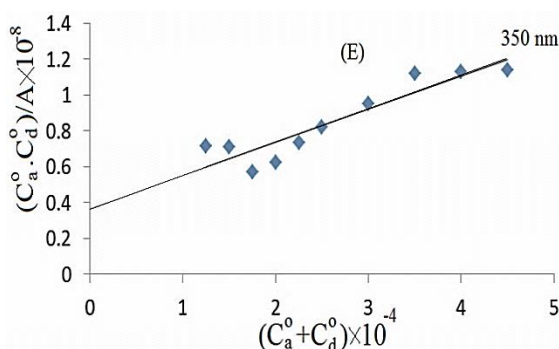


(B): OLP-HPA reaction in MeOH at 354 nm

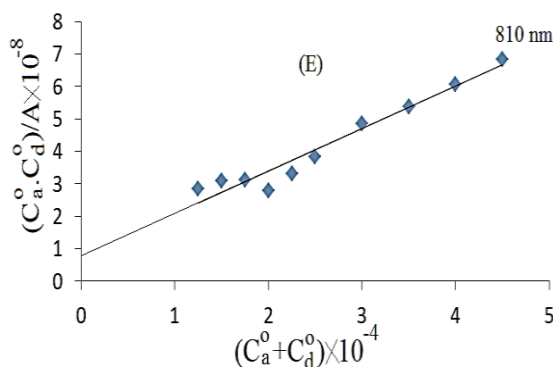
(C): OLP-H₂CA reaction in MeOH at 305 nm



(D): OLP-DNS reaction in MeOH at 310 nm

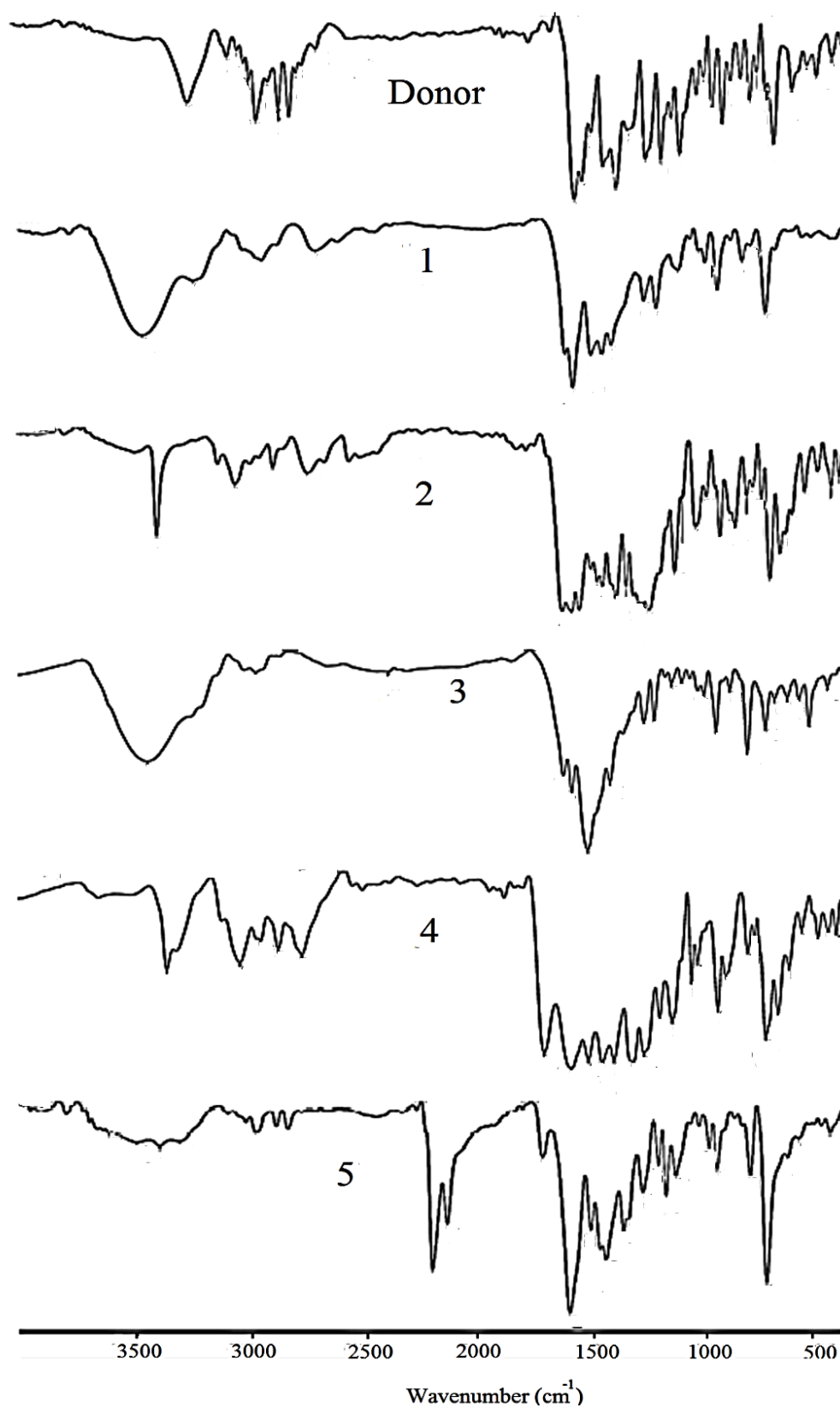


(E): OLP-TCNQ reaction in MeOH at 350



(E): OLP-TCNQ reaction in MeOH at 810 nm

Fig 4. IR spectra of OLP and its CT-complexes



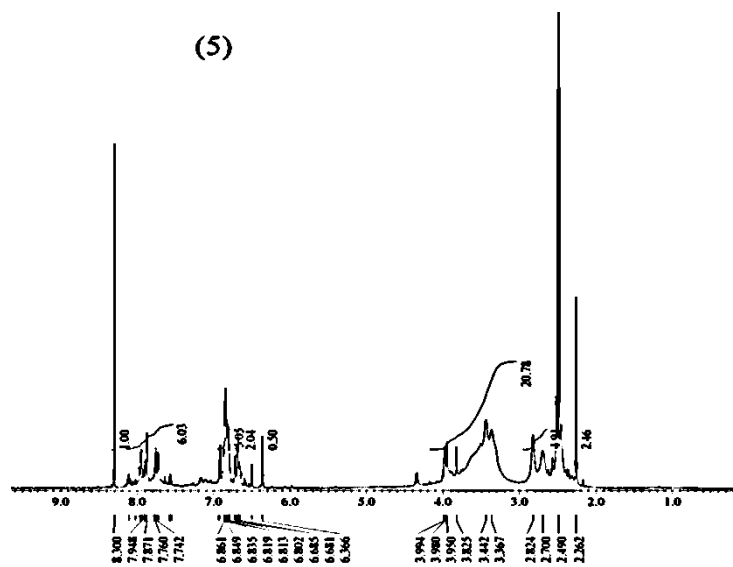
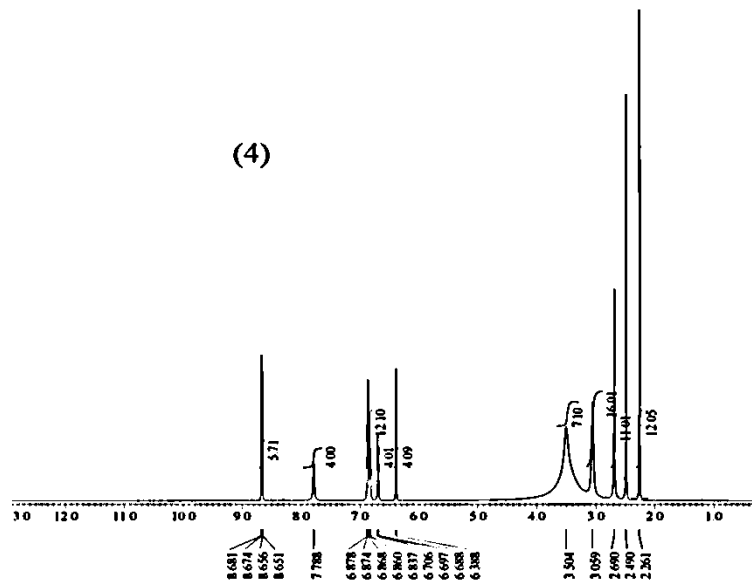
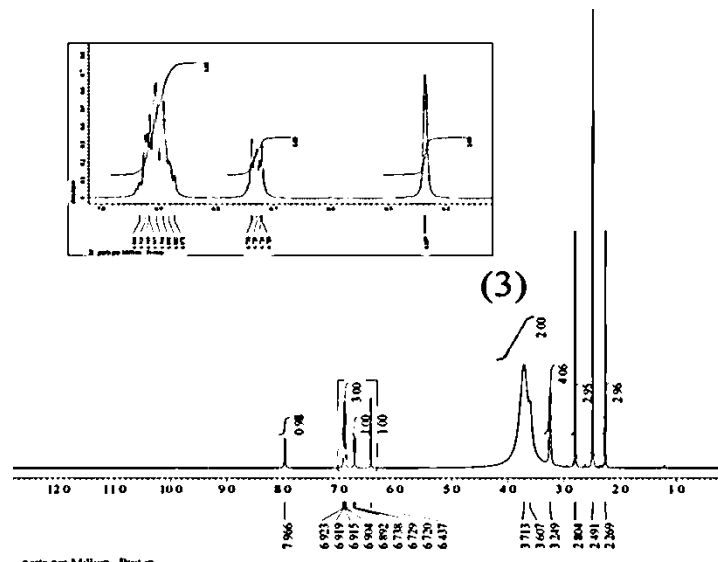
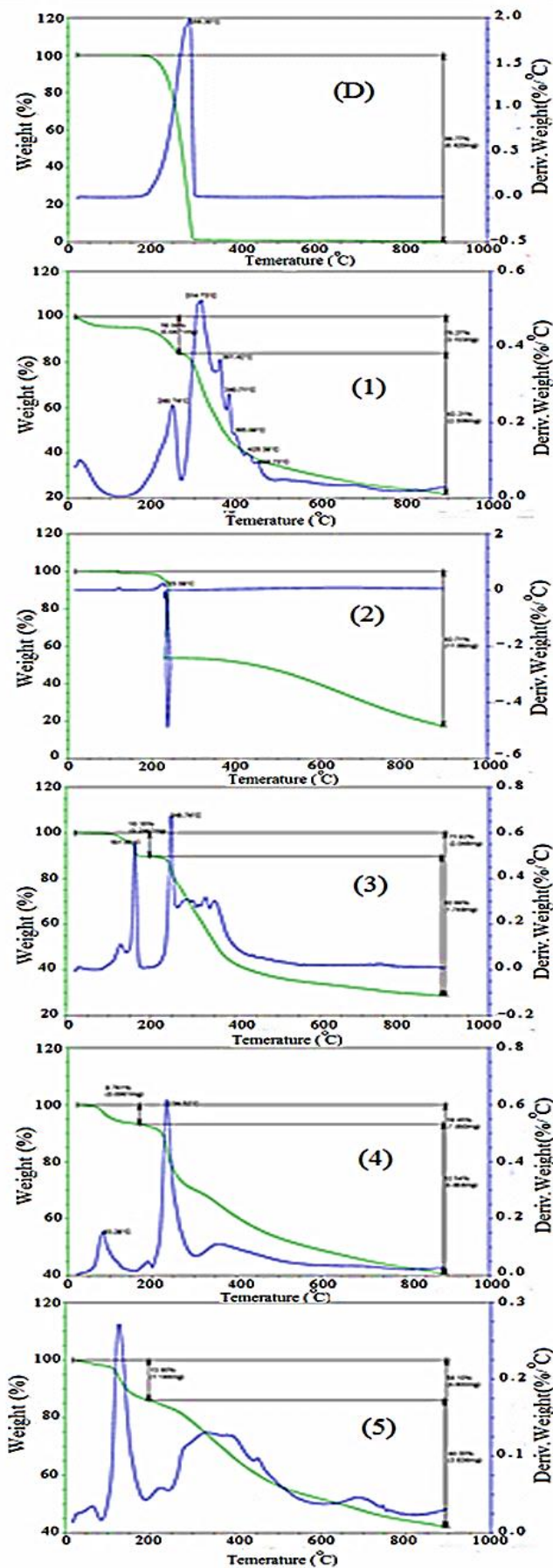


Fig 6. Thermogravimetric (TGA) and derivative (DTG) of OLP and its complexes



REFERENCES

- [1] A.A. Adam, H.H. Eldaroti, M.S. Hegab, M.S. Refat, J.H. Al-Humaidi, H.A. Saad, *Spectrochim Acta Part A: Mol and Biomol Spect.* 211 (2019) 166–177.
- [2] I.M. Khan, A. Ahmad, M.F. Ullah, J. *Photochem. Photobio. B: Bio* 103 (2011) 42–49.
- [3] A.S. Gaballa, S.M. Teleb, E. Rusanov, D. Steinborn. *Inorganic Chimica Acta* 357 (2004) 4144–4150.
- [4] L. Shahada, A. Mostafa, E. Nour, H. S. Bazzi, *J. Mol. Struct.* 933 (2009) 1–7.
- [5] I.M. Khan, A. Ahmad, *J. Mol. Struct.* 975 (2010) 381–388.
- [6] E M. Nour, S. Y. AlQaradawi, A. Mostafa, E. Shams, H. S. Bazzi, *J. Mol. Struct.* 980 (2010) 218–224.
- [7] D. Nanova, S. Beck, A. Fuchs, T. Glaser, C. Lennartz, W. Kowalsky, A. Pucci, M. Kroeger, *Organic Electronics* 13 (2012) 1237–1244.
- [8] A.A. Adam, *Spectrochim. Acta A Mol. and Biomol. Spect.* 104 (2013) 1–13.
- [9] A.S. Gaballa; *J. Chem. Pharm. Research*, 7(4) (2015) 431–446.
- [10] D.K. Roy, A. Saha, A.K. Mukherjee, *Spectrochim. Acta A* 61 (2005) 2017–2022.
- [11] A.M. Slifkin, *Charge-Transfer Interaction of Biomolecules*, Academic Press, New York, 1971.
- [12] A. Dozal, H. Keyzer, H.K. Kim, W.W. Wang, *Int. J. Antimicrob. Agent* 14 (2000) 261.
- [13] A. Korolkovas, *Essentials of Medicinal Chemistry*, 2nd Edn., Wiley, New York, USA, 1998 (Chapter 3).
- [14] F. Yakuphanoglu, M. Arslan, *Solid State Commun.* 132 (2004) 229–234.
- [15] F. Yakuphanoglu, M. Arslan, *Opt. Mater.* 27 (2004) 29–37.
- [16] F. Yakuphanoglu, M. Arslan, M. Kucukislamoglu, M. Zengin, *Sol. Energy* 79 (2005) 96–100.
- [17] L. Chelkeba, K. Gidey, A. Mamo, B. Yohannes, T. Matso, T. Melaku. *Pharm. Pract. (Granada)*. 2017 Jan-Mar;15(1):877.doi:10.18549/PharmPract.2017.01.877. Epub 2017 Mar 15. [PubMed:28503222].
- [18] K.S. Rubesh, P. Gayathri, N. Duganath, C.H. Kiran, C. Sridhar, K. Jayaveera, *Int. J. Pharm. Sci. Drug Res.* 3 (2011) 52–55.
- [19] European Medicines Agency, *Pre-authorisation Evaluation of Medicines for Human Use. Assessment Report for Zypadhera (International Nonproprietary Name: olanzapine)*, 2008.
- [20] D.A. Skoog, *Principle of Instrumental Analysis*, 3rd Edn, Saunders, New York, USA, 1985 (Chapter 7).
- [21] D.J. Beecher, A.C. Wong, *Appl. Microbiol.* 60 (1994) 4614–4616.
- [22] National Committee for Clinical Laboratory Standards. *Methods for Antimicrobial Susceptibility Testing of Anaerobic Bacteria: Approved Standard M11 A3*. NCCLS, Wayne, PA, USA, 1993.
- [23] A.W. Bauer, W.M. Kirby, C. Sherris, M. Turck, *Am. J. Clin. Pathol.* 45 (1966) 493.
- [24] S.Y. AlQaradawi, H.S. Bazzi, A. Mostafa, E.M. Nour, *J. Mol. Struct.* 998 (2011) 126–135.
- [25] R. Abou-Ettah, A. El-Korashy, *J. Phys. Chem.* 76 (1972) 2405.
- [26] H. Tsubomura, R. P. Lang, *J. Am. Chem. Soc.* 83 (1961) 2085.
- [27] R. Rathore, S.V. Lindeman, J.K. Kochi, *J. Am. Chem. Soc.* 119 (1997) 9393.
- [28] G. Aloisi, S. Pignataro, *J. Chem. Soc., Faraday Trans.* 69 (1972) 534.
- [29] G. Briegleb, *Z. Angew. Chem.* 72 (1960) 401; G. Briegleb, *Z. Angew. Chem.* 76 (1964) 326.
- [30] R. Abu-Eittah, F. Al-Sugeir, *Can. J. Chem.* 54 (1976) 3705.
- [31] M.S. Refat, *J. Mol. Struct.* 985 (2011) 380–390.
- [32] I.M. Khan, A. Ahmad, S. Kumar, *J. Mol. Struct.* 1035 (2013) 38–45.
- [33] S.M. Teleb, A.S. Gaballa, M.A.F. Elmosallamy, E.M. Nour, *Spectrochim. Acta A* 61(11–12) (2005) 2708–2712.
- [34] A.S. Gaballa, C. Wagner, S.M. Teleb, E. Nour, M.A.F. Elmosallamy, G. N. Kalud-erovic, H. Schmidt, D. Steinborn. *J. Mol. Struct.* 876 (2008) 301–307.
- [35] I.M. Khan, S. Shakya, N. Singh, *J. Mol. Liq.* 250 (2018) 150–161.
- [36] M.M. Ali, A.S. Gaballa, R.A. Haggan, N.A. Elkhosy and S.M. Teleb; *J. Chem. Pharm. Research* 6(11) (2014) 570–580.
- [37] A.S. Gaballa, S.M. Teleb, E. Nour, *J. Mol. Struct.* 1024 (2012) 32.
- [38] K. Alam, I.M. Khan, *Organic Electron* 63 (2018) 7–22.
- [39] M.M. Ali, A.S. Gaballa, S.M. Teleb, *Russian J. Gen. Chem.* 85(3) (2015) 731–745.
- [40] M. Pandeewaran, K.P. Elango *Spectrochim Acta A* 75 (2010) 1462–1469.
- [41] O. Saoudi, S. M. Teleb, and A. S. Gaballa, *Russian J. Gen Chem*, 88 (2018) 797–803.
- [42] A. Mostafa, N. El-Ghossein, G. B. Cieslinski, Hassan S. Bazzi, *J. Mol. Struct.* 1054–1055 (2013) 199–208.
- [43] A.A. Adam, H. Eldaroti, M.S. Refat, H.A. Saad, *J. Mol. Struct* 1037 (2013) 376–392.
- [44] J Šesták; P Šimon, Editors. *Thermal Analysis of Micro, Nano-and Non-Crystalline Materials*. Springer Science+Business Media Dordrecht, 2013.